

Implication of long-distance cytoplasmic transport into dynamics of local pH on the surface of microinjured *Chara* cells

Alexander A. Bulychev¹ · Anna V. Komarova¹

Received: 22 March 2016 / Accepted: 13 April 2016 / Published online: 18 April 2016
© Springer-Verlag Wien 2016

Abstract Cytoplasmic streaming is essential for intracellular communications but its specific functions are not well known. In *Chara corallina* internodes, long-distance interactions mediated by cyclosis are clearly evident with microscopy-pulse amplitude modulation (PAM) fluorometer under application of localized light (LL) pulses to a remote cell region. Measurements of LL-induced profiles of chlorophyll fluorescence F' at various distances from the LL source suggest that illuminated chloroplasts release into the streaming cytoplasm excess reducing equivalents that are entrained by the fluid flow and transiently reduce the intersystem electron carriers in chloroplasts of downstream shaded areas. The reducing equivalents propagate to distances up to 4.5 mm from the LL source, with the transport rate nearly equal to the velocity of liquid flow. The F' transients disappeared after the arrest of streaming with cytochalasin D and reappeared upon its recovery in washed cells. The F' responses to a distant LL were used as an indicator for the passage of cytosolic reductants across the analyzed cell area during measurements of cell surface pH (pH_o) in intact and microperforated internodes. In microwounded cell regions, the LL-induced increase in F' occurred synchronously with the increase in pH_o , by contrast to a slight decrease in pH_o observed prior to perforation. The results show that reducing agents transported with the cytoplasmic flow are involved in rapid pH changes on the surface of microinjured cells. A possibility is considered that cytoplasmic reductants are processed by stress-activated plasmalemmal

NADPH oxidase carrying electrons to oxygen with the eventual H^+ consumption on the outer cell side.

Keywords Long-distance communications · Microfluorometry · Cytoplasmic streaming · Cytochalasin D · Cell wall microperforation · Proton flows

Abbreviations

AOI	Area of inspection (area of interest)
CW	Cell wall
LL	Localized lighting (localized light)
PFD	Photon flux density
pH_o	pH on the cell surface

Introduction

Fundamental biological properties of plant cells, such as intracellular motility, excitability, photosynthesis, and the formation of steady-state structures, are clearly pronounced in characean algae, the close relatives of higher plants (Allen and Allen 1978; Toko et al. 1985; Shimmen 2007; Beilby and Bisson 2012). Because of evolutionary similarity of charophytes and terrestrial plants in terms of their cell structures and metabolism (Beilby and Casanova 2014) and owing to large dimensions of internodes, the characean internodal cells represent a convenient model for studying the interactions of basic cell processes in vivo. Such a model is particularly attractive for examining the interrelation of photosynthesis and membrane transport in intact cells (Bulychev and Kamzolnikina 2006; Krupenina et al. 2008), where the regulatory links are much more diverse and complex than in isolated organelles.

Handling Editor: Peter Nick

✉ Alexander A. Bulychev
bulychev@biophys.msu.ru

¹ Faculty of Biology, Lomonosov Moscow State University, 119992 Moscow, Russia

Large dimensions of characean internodes necessitate the existence of specific cell mechanisms essential for the survival of aquatic macrophytes. Unlike in small-sized cells, where reagents come into contact by diffusion, in characean internodal cells measuring up to ≥ 10 cm, diffusion is ineffective as a means of intracellular communication (Verchot-Lubicz and Goldstein 2010; Goldstein and van de Meent 2015). The integration of cell metabolism and the transmission of intracellular messages is largely due to the cytoplasmic rotational streaming (Pickard 2003) whose velocity can be as high as $100 \mu\text{m s}^{-1}$. Continuous exchange of metabolites across the chloroplast envelope (Foyer and Noctor 2009; Taniguchi and Miyake 2012) under natural fluctuating nonuniform light (Pearcy et al. 1996; Leakey et al. 2005) generates lateral gradients of substrates and signaling molecules in the cytoplasm, which results in the translocation of these metabolites in the direction of cytoplasmic flow (Bulychev and Dodonova 2011). Chloroplasts exposed to strong light modify the composition of streaming cytoplasm, while the components carried by liquid flow exert their influence on chloroplasts in shaded cell areas far away from the illuminated spot (Bulychev and Komarova 2015). Cyclosis not only supports long-distance interactions between chloroplasts but also conveys the intermediates from chloroplasts to the plasmalemmal transport systems, which results in pH changes at the cell surface at various distances from the illuminated area (Dodonova and Bulychev 2011).

Another important strategy for the survival of large-sized cells in coenocytic algae consists in healing the microscopic wounds because wounding of large cells may result in the loss of a considerable part of whole plant biomass (Foissner 1988; Menzel 1988). The repair of pointed injury is likely to implicate the cyclosis-dependent lateral transport of intracellular resources to the wounded region from areas located beyond the point of injury (Hardham et al. 2007; Klima and Foissner 2011). However, the data on the role of cytoplasmic streaming in cell responses to the pointed mechanical stimuli are rather scarce.

The microscopic damage of a cell wall, the first cell barrier, might be associated with the release of chemical constituents perceived by membrane receptors (Heil 2009). In addition, it may directly activate mechanosensitive ion channels (Monshausen et al. 2009). After local weakening of *Chara* cell wall by pointed perforation with a glass microneedle, the high internal hydrostatic pressure seems to press the plasma membrane into the defect of rigid support, which is followed by membrane extension, opening of stretch-activated Ca^{2+} channels, and the entry of Ca^{2+} from the external medium into the cytoplasm (Bulychev et al. 2013a). The localized increase in the cytoplasmic Ca^{2+} level mediates the subsequent local increase in external pH (pH_0) by 2–3 units compared to the pH in the bulk medium. Sharp alkalization of the medium in the vicinity of incision, concurrent with the acidification of

cytosol, is considered as a transmembrane H^+ redistribution serving to strengthen the cell wall (Monshausen et al. 2009). The alkaline domains produced by microincision are similar in pH level to the alkaline zones arising under whole-cell or localized illumination. However, they remained unnoticed for a long time because the area of such domains is approximately two orders of magnitude lower than the area of natural light-dependent pH domains. Despite the seeming similarity, the incision-induced alkaline domains differ from the light-dependent alkaline zones in terms of sensitivity to intracellular Ca^{2+} increase associated with the action potential generation (Bulychev and Komarova 2014). The membrane excitation (action potential) clearly stimulated the pH response to microperforation but transiently eliminated the pH zones produced by intact cells in the light (Krupenina and Bulychev 2007; Krupenina et al. 2008). These distinctions point to the specificity of the membrane system responsible for the drastic pH increase on the cell surface after microincision. However, the mechanism of such alkaline pH shift and the possible involvement of cyclosis in this event are not yet determined.

The role of cytoplasmic streaming in cell responses to microperforation could be clarified by tracking the changes of chloroplast actual fluorescence F' and the cell surface pH upon localized illumination of a remote cell region. In this study, by measuring modulated chlorophyll fluorescence on microscopic regions of *Chara* internodal cells, we first demonstrate the downstream propagation of photosynthetically active intermediate from the locally illuminated cell area in the direction of cytoplasmic flow. A closer inspection of cyclosis-mediated F' changes in response to localized illumination of a remote cell region revealed that the F' profiles depend on the streaming velocity and disappear in the absence of streaming. Finally, we show that the metabolite transported with the cytoplasmic flow participates in early physicochemical events initiated by microperforation of the cell wall. The results provide evidence for the involvement of cytoplasmic streaming and plasmalemma-mediated oxidation of cytoplasmic reductants in the cell response to microwounding.

Materials and methods

Plant material

Chara corallina algae were grown in 50-L glass vessels at room temperature under scattered daylight (photosynthetic photon flux density $\sim 10 \mu\text{mol m}^{-2} \text{s}^{-1}$ during daytime). Isolated internodal cells measuring 6–8 cm in length and about 0.9 mm in diameter were placed into artificial pond water containing 0.1 mM KCl, 1.0 mM NaCl, and 0.1 mM CaCl_2 . The medium was supplemented with NaHCO_3 to adjust the pH at 7.0. Prior to experiments, the cell was mounted in a transparent organic glass chamber with a total bath volume

of 40 mL and placed on a stage of an inverted fluorescence microscope Axiovert 25-CFL (Zeiss, Germany). Microscopic observations and fluorescence measurements were made on the lower cell side. The chloroplasts in characean internodes are anchored; they are arranged in slightly twisted rows extending along the streamlines of fluid flow and subcortical actin filaments (Shimmen 2007; Foissner and Wasteneys 2012). Experiments were mostly made on cell regions with comparatively high photosynthetic activity, where pericellular external pH (pH_o) becomes slightly acidic under bright light. The localized illumination was applied to cell regions positioned either upstream or downstream in the cytoplasmic flow with respect to the area of inspection (AOI) where chlorophyll fluorescence was assayed. The velocity of cytoplasmic movement in untreated cells was $60\text{--}90\ \mu\text{m s}^{-1}$ as measured with a stopwatch.

Continuous measurements of modulated fluorescence

The counter-directed cytoplasmic flows in *Chara* internodes occur on diametrically opposite cell sides that are separated by distances up to $1000\ \mu\text{m}$. At a sufficiently high numerical aperture of the objective lens, the depth of field does not exceed few micrometers. Therefore, fluorescence can be selectively measured for chloroplasts residing on the lower cell side where the direction of streaming is well defined.

Parameters of chlorophyll fluorescence *in vivo* were measured on microscopic cell regions (diameter $\sim 100\ \mu\text{m}$) using a microscopy-pulse amplitude modulation (PAM) fluorometer (Walz, Germany) equipped with a $\times 32/0.4$ objective lens. The majority of data represent continuous changes in actual fluorescence F' emitted under dim background illumination of the whole cell (operation mode “Ft only”). The signal from a photomultiplier was fed into the PAM control unit of pulse-amplitude modulation system, digitized by means of an AD converter PCI-6024E (National Instruments, USA), and displayed on a computer monitor using WinWCP program (Strathclyde Electrophysiology Software). Data points were sampled at regular intervals of about 51 ms.

Background and localized illumination

The excitation/emission light beams used for microfluorometry, the position of an optic fiber employed for localized photostimulation of a distant cell area, and the background illumination of the whole internode were configured as shown schematically in a previous work (Bulychev et al. 2013b).

The background illumination of the whole cell was provided from a microscope upper light source through a 5-mm-thick blue glass filter SZS-22 ($\lambda < 580\ \text{nm}$). The incident photon flux density (PFD) from this light source was determined with a spherical micro quantum sensor US-SQS connected to a

PAM control unit (Walz). The intensity of background illumination was attenuated by neutral density glass filters. In the major part of experiments, the PFD incident on the upper cell side was approximately $9\ \mu\text{mol m}^{-2}\ \text{s}^{-1}$. At this dim irradiance, the pH bands were mostly absent. However, this background illumination sufficed for the appearance of alkaline bands near the light–shade border under localized illumination of a preselected cell region.

The localized illumination (localized light, LL) was applied through a thin quartz optic fiber to cell regions located at various distances from the point of measurements (AOI). The optic fiber with a diameter of $400\ \mu\text{m}$ was connected to a source of white light (a light-emitting diode Luxeon LXX2-PWN2-S00, Lumileds, USA). The PFD at the output of the light guide equaled to $500\ \mu\text{mol m}^{-2}\ \text{s}^{-1}$. In order to reduce the number of intermediates exchanged between the chloroplasts and cytoplasm in the area of localized illumination, comparatively short (30–50 s) pulses of LL were used in most experiments. Longer LL pulses were needed for generation of alkaline bands near the light–shade border. The free end of the light guide was fixed in the holder of a mechanical KM-1 micromanipulator (Chernogolovka, Russia) under the angle of $30\text{--}45^\circ$ to a horizontal plane. After adjusting the light guide position in the view field near the cell, the optic fiber was displaced with a micrometric screw to distances from 1 to 4.5 mm upstream the cytoplasmic flow with respect to the analyzed region.

Measurements of surface pH and microperforation

The local pH on the outer cell surface (pH_o) was measured with glass-insulated antimony pH-microelectrodes having tip diameters of $5\text{--}15\ \mu\text{m}$. The slope of the electrode function was approximately $54\ \text{mV/pH}$ unit. Microperforation of the cell wall (CW) was accomplished using glass micropipettes with a tip size of $\sim 1\ \mu\text{m}$; the pipettes were pulled from Pyrex glass capillaries having an outer diameter of 1.1 mm. The experiments were usually performed in photosynthetically active areas that would produce acid zones under elevated light intensities.

The cell surface pH was recorded at a distance of $\leq 10\ \mu\text{m}$ from the point of CW microperforation. Chlorophyll fluorescence was measured at the nearest place to the point of incision, with an objective lens focused on the bottom chloroplast layer. The experimental setup allowed independent positioning of four microtools (Bulychev and Komarova 2016): the pH microelectrode, the micropipette for CW perforation, a supporting glass capillary to prevent cell displacement during microincision, and a fiber optic for directing LL to the remote cell region.

Cytochalasin D (Sigma) was kindly provided by Prof. I. Foissner (University of Salzburg). A stock solution was

prepared with DMSO (10 mM) and diluted to final concentrations of 10 and 25 μM with the standard medium.

Figures represent the results of representative experiments performed in at least four replicates with different cells. Traces in figures are either individual or averaged curves calculated from several records, with n indicating the number of replicate measurements.

Results

Downstream propagation of chlorophyll fluorescence transients

Figure 1 shows changes in chlorophyll fluorescence F' induced by a pulse of LL ($500 \mu\text{mol m}^{-2} \text{s}^{-1}$, pulse duration 30 s, beam diameter $400 \mu\text{m}$) that was applied at various distances from the analyzed cell region when the whole cell was exposed to weak background light ($\sim 8 \mu\text{mol m}^{-2} \text{s}^{-1}$, $\lambda < 580 \text{ nm}$). Once the area of inspection (AOI) was selected, its position was kept constant throughout the experiment, while the distance d between AOI and LL spot was adjusted by displacing the optic fiber along the internode axis.

In the shaded cell regions, upward fluorescence changes were only observed on the downstream side from LL with regard to the direction of cytoplasmic streaming. These changes having a roughly symmetric shape could be fitted with

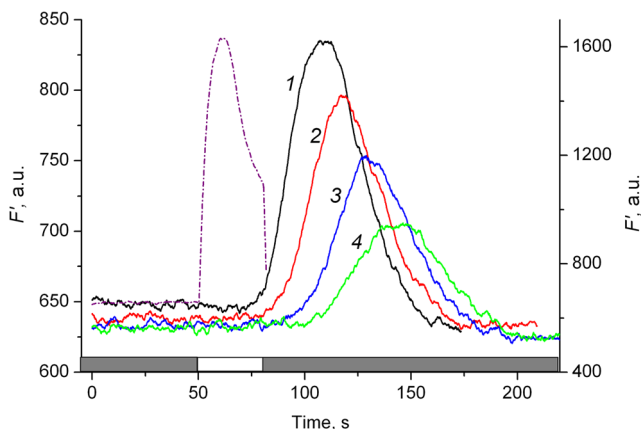


Fig. 1 Transient changes in chlorophyll fluorescence F' induced by localized illumination (LL, white light, $500 \mu\text{mol m}^{-2} \text{s}^{-1}$, pulse duration 30 s, beam diameter $400 \mu\text{m}$) of a remote cell region, as measured at distances d of 1, 1.5, 2, and 2.5 mm downstream from the illuminated spot (curves 1–4, respectively). The whole cell was exposed to weak background light ($8 \mu\text{mol m}^{-2} \text{s}^{-1}$, $\lambda < 580 \text{ nm}$). The *dashed line* associated with the right-side (coarse) scale shows the changes in F' fluorescence occurring directly in the cell region illuminated by LL ($d = 0$). The *white and gray bars* along the x axis show the timing of LL application. An abbreviation *a.u.* in this and other figures means arbitrary units

Gaussian curves. As the gap distance d was increased, the lag time preceding the peak of F' band was prolonged. In addition, a slight widening of the Gaussian curve was noticed. The broken line associated with the right y -axis in Fig. 1 shows on a coarser scale fluorescence changes occurring directly in the illuminated cell region. The fluorescence induction curve in a brightly illuminated area comprised a steep fluorescence rise to the peak and a subsequent slower non-photochemical quenching of fluorescence, in accordance with the commonly known temporal transients in leaves and algae. The shape of fluorescence transients in brightly illuminated region differed distinctly from those in shaded cell regions.

The serial profiles of F' changes in response to localized illumination of a remote cell region, as recorded at various distances from the LL source, can be used to visualize the propagation of F' transients in the direction of cytoplasmic flow. Figure 2a shows a three-dimensional image, where fluorescence intensity was plotted as a function of distance d from the LL source and as a function of current time t from the onset of recording. A 30-s pulse of LL was applied at $t = 50 \text{ s}$. As the gap distance d was enlarged, the peak in F' transients was lowered and developed with a longer delay. Figure 2b displays, for another experiment, a two-dimensional time–space plot, where fluorescence intensity is color-coded and presented as a function of the same variables, namely, the gap distance between the centers of illuminated and analyzed cell regions and the recording time. The result suggests that the active metabolite or regulating factor released into the cytoplasm in the area of intense illumination travels for distances at least 4.5 mm. The inverse of the slope of a straight line drawn through the F' peak positions at various time instants corresponds to the rate at which the active intermediate is transported; in the experiment shown in Fig. 2b, this rate was $53 \mu\text{m s}^{-1}$. It should be noted that the spatial coordinate in Fig. 2 represents the axial distance along the cell length, whereas the distance covered by the flowing cytoplasm was higher by a factor of approximately 1.25 because the cytoplasm moved along the helical path with a pitch of $\sim 12 \text{ mm}$ and a diameter of about 0.95 mm . When the helical trajectory was taken into account, the translocation rate for the photosynthetically active metabolite increased to $66 \mu\text{m s}^{-1}$, which corresponded to the actual velocity of cytoplasmic streaming in that experiment.

It is seen in Fig. 2b that the F' level undergoes wavelike changes along the internode length. For example, in 60 s after switching off LL (at $t = 140 \text{ s}$ from the onset of recording), fluorescence changes at a distance $d = 1 \text{ mm}$ from the LL source were completed, whereas at a distance of 4.5 mm, the F' fluorescence just attained the peak. The wavelike F' transients reflect the vectorial movement of the active intermediate along with the liquid flow.

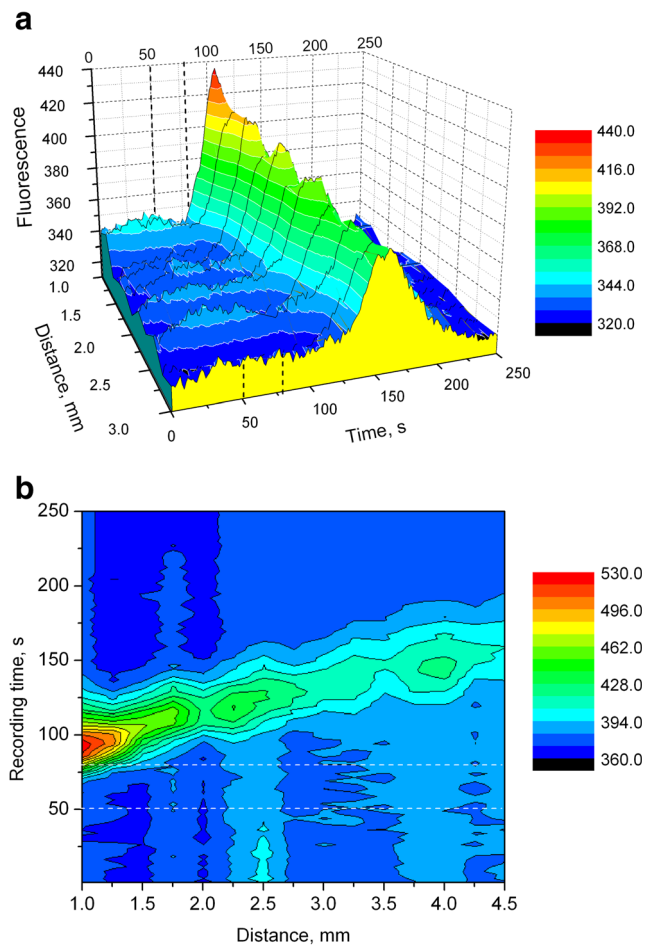


Fig. 2 Spatiotemporal changes in F' fluorescence on the downstream side of the remote cell region exposed to LL. **a** Three-dimensional plot showing the wavelike propagation of F' transients along the cell length. Distance is counted from the center of intense localized illumination (LL). Zero time corresponds to the onset of F' recording. The LL pulse of 30 s duration was applied at $t=50$ s; this interval is marked by vertical *dashed lines* on the front and rear side panels. Background light intensity, $9 \mu\text{mol m}^{-2} \text{s}^{-1}$. **b** Two-dimensional time–space diagram of F' transients induced by LL applied to a remote cell region. The *color codes* indicate the fluorescence intensity. Horizontal white lines mark the time interval at which LL was switched on. Background light intensity, $9 \mu\text{mol m}^{-2} \text{s}^{-1}$

Superposition of opposite F' changes at the light–shade border

Measurements of F' fluorescence at a distance d of 1 mm from the center of illuminated cell region ($800 \mu\text{m}$ from the light–shade border) revealed that the stage of fluorescence rise is often preceded by a steep decrease in light emission following the application of a remote LL pulse (Fig. 3, curve 1). Such a decrease in F' cannot be caused by scattered light because even a slight increase in background illumination enhanced F' fluorescence. Analogous, though a weaker decrease in F' was also observed at a distance of 1 mm on the upstream side from the LL position (curve 2). This transient was hardly noticed at $d=1.5$ mm and absent at larger distances d . The

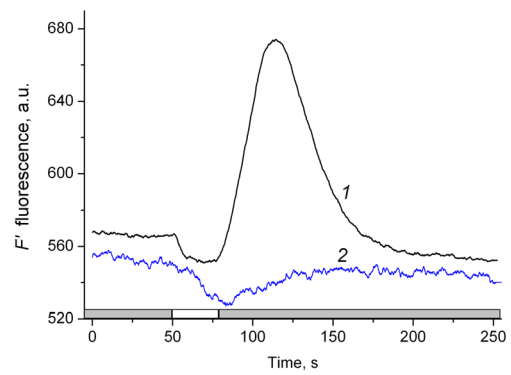


Fig. 3 Fluorescence F' transients caused by localized illumination at a 1-mm distance d from the center of LL application. Duration of LL pulse was 30 s; background light intensity, $8 \mu\text{mol m}^{-2} \text{s}^{-1}$. Traces 1 and 2 are F' changes measured on the downstream and upstream sides, respectively, from the center of localized illumination. Curve 1 is an average trace obtained from 15 records on three cells. *White and gray bars* along the x axis show the timing of LL application

decrease in F' near the light–shade margin seems to develop too fast to be directly caused by cyclosis. It might represent non-photochemical quenching related to the passage of circulating electric current between illuminated and shaded areas of the internodal cell. The incidence of a narrow light beam is known to promote H^+ extrusion and acidify the unstirred water layer in the illuminated area, while the adjacent shaded areas become the sink for protons entering the cytoplasm. A narrow dimly lit region near the light–shade border was a particular site where the peak of F' was preceded by fluorescence quenching. The origin of rapid fluorescence quenching at a comparatively small distance from the illuminated spot could be a matter of a separate study.

Lateral transport and diffusion of photosynthetically active intermediate

The increase in fluorescence F' at large distances from the illuminated cell region presumably involves a series of events, including the export of reducing equivalents (NADPH) from chloroplasts in the brightly illuminated area, the downstream transport of reducing equivalents with the cytoplasmic flow, the entry of reductants into the stroma of shaded chloroplasts, and the eventual reduction of plastoquinone and the quinone acceptor Q_A in photosystem II (Bulychev and Komarova 2015). If low-molecular-weight metabolites remain free during lateral transport, they would diffuse along the cell length and widen the F' spatial profile. The diffusion-related widening of the F' profile should be particularly evident under low velocity of cytoplasmic streaming. Under these conditions, diffusion proceeds over a longer period during which the cytoplasmic portion enriched with reducing equivalents covers a fixed distance from the point of LL to AOI.

We verified these predictions by measuring the profiles of F' fluorescence changes induced by LL treatment of a remote

cell region after various periods of internode incubation in the presence of an actin inhibitor, cytochalasin D. This inhibitor reversibly suppresses cytoplasmic streaming without appreciable influence on photosynthetic electron transport in chloroplasts (Sommer et al. 2015). Figure 4a shows the profiles of F' responses to remote LL at a fixed distance $d=1.5$ mm under normal and decelerated velocities of cytoplasmic streaming before and during the cytochalasin D treatment (10 μ M). It is seen that the retardation of cyclosis not only delayed the

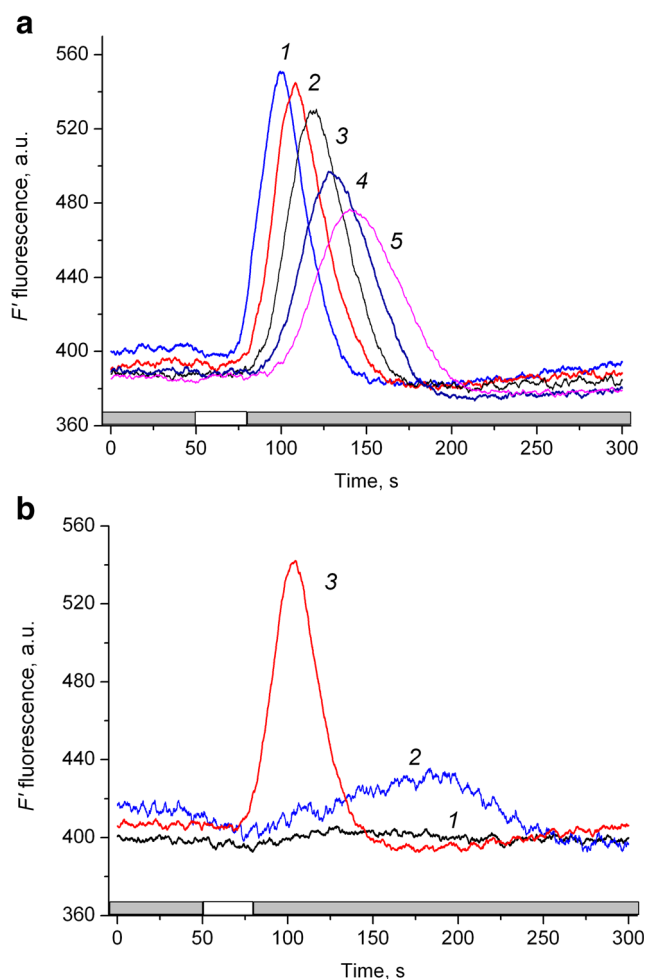


Fig. 4 Modifications of cyclosis-mediated F' response at a fixed distance d from the remote LL source during deceleration of cytoplasmic streaming by cytochalasin D treatment and after the recovery of streaming in a washed cell. Background light intensity, $9.8 \mu\text{mol m}^{-2} \text{s}^{-1}$. **a** Retardation of streaming velocity during incubation of *C. corallina* internode in the presence of 10 μM cytochalasin D was accompanied by the delayed appearance of the F' peak and by broadening the bandwidth of F' transients. Curves 1–5 are averaged data obtained from three to eight records each. Mean velocities of cytoplasmic streaming were 75, 60, 36, 24, and 18 $\mu\text{m s}^{-1}$ for curves 1–5, respectively. **b** Disappearance of F' transients after the arrest of cytoplasmic streaming by 25 μM cytochalasin D in the same cell as in Fig. 4a, and restoration of fluorescence changes during the recovery of streaming in washed cells. 1—in the absence of streaming, 2—shortly after the removal of cytochalasin D, when the streaming velocity ranged from 5 to 12 $\mu\text{m s}^{-1}$, 3—complete restoration of streaming after washing the cell for ≥ 40 min. Curves 1 and 3 are averaged data ($n=4$), 2 is an individual record

appearance of F' peak but also extended the bandwidth of F' transients. Remarkably, the area under the bell-shaped curves remained almost identical during the retardation of cyclosis.

Elevation of cytochalasin D concentration in the incubation medium from 10 to 25 μM completely arrested the cytoplasmic streaming. Under these conditions, the F' transients in response to the remote LL stimulus disappeared (Fig. 4b, curve 1). After washing the cell from the inhibitor with the fresh medium, both the cytoplasmic streaming and the fluorescence responses to LL were restored (curves 2, 3). The streaming velocity recovered to approximately 70 % of its initial value in 20 min after the removal of cytochalasin D, whereas an almost complete restoration was attained after 40 min. A similar period of streaming recovery was observed on internodal cells of *Nitella pseudoflabellata* after replacing a 60 μM cytochalasin D solution with artificial fresh water (Foissner and Wasteneys 2007).

Involvement of lateral transport in the dynamics of surface pH in microperforated cells

The plant cell responses to mechanical stimuli and wounding are known to involve the plasma-membrane NADPH oxidase that transfers electrons from cytoplasmic NAD(P)H to extracellular oxygen (Suzuki et al. 2011). The transmembrane electron flow to O_2 , with or without formation of reactive oxygen species, might be accompanied by the buildup of ΔpH and the pH increase on the outer side of the plasma membrane. In order to test a possible involvement of the lateral transfer of reducing equivalents in surface alkalization after cell wall incision, we performed simultaneous measurements of pH and chlorophyll fluorescence near the point of microperforation under localized illumination of a distant cell region.

Figure 5a shows the incision-induced changes in surface pH, as well as changes in F' chlorophyll fluorescence caused by localized illumination of the remote cell region positioned upstream in the liquid flow. Microperforation of CW with the tip of a glass microneedle elevated the local pH by approximately 3–3.5 units after a lag period ~ 10 s; this sharp alkalization was followed by a slow decrease in pH. The application of LL pulses to a cell region located 1.5 mm on the upstream side from AOI resulted in the transient increase in F' , as described above. The influence of LL on pH_o was either lacking or inconspicuous at this stage. However, later in the experiment, after about 10 min from the sharp alkalization, when the pH lowered gradually at the point of microincision, the pH changes induced by LL became larger. Furthermore, the temporal coincidence of LL-induced pH shifts and F' increase became evident (Fig. 5b). Considering that slight pH changes occurred on the background of a gradual pH decline, we plotted the graphs for the first derivative of the pH changes. The maxima of the first derivative, dpH/dt coincided with the positions of the F' peaks (Fig. 5c). Thus, the maximal rate

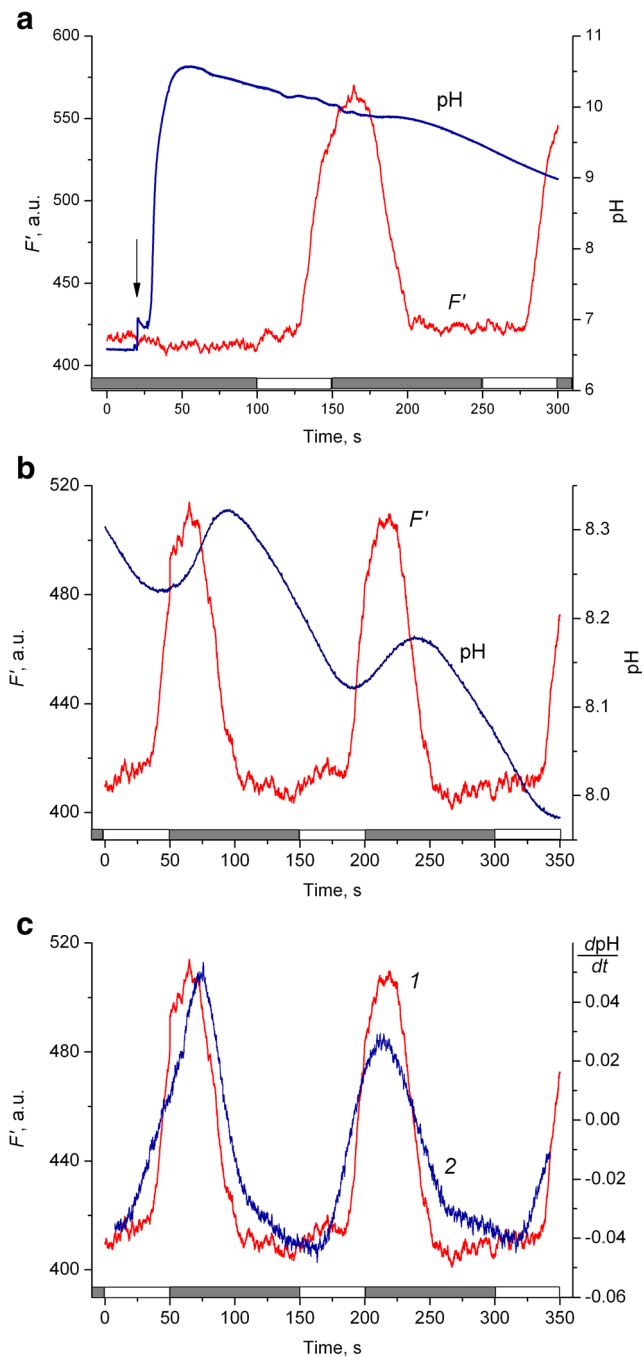


Fig. 5 Simultaneous recording of chlorophyll fluorescence F' and pH_o near the microperforated region under localized illumination of a remote cell site positioned 1.5 mm upstream from the analyzed area. *White and gray bars* along the x axis show the timing of intermittent 50-s pulses of LL applied to a remote cell area. Background light intensity, $9 \mu\text{mol m}^{-2} \text{s}^{-1}$. **a** The increase in pH_o caused by cell wall incision with a glass micropipette (*arrow*) and responses of F' fluorescence to intermittent local lighting in the absence of significant pH_o changes at a high pH_o level. **b** Concurrent changes in F' and pH_o in response to LL of the remote cell region, occurring on the background of decreasing pH_o in the wounded area. **c** Synchronous cyclosis-mediated increases in F' fluorescence (1) and the first derivative of the outer pH in the area of cell wall microperforation (2). The pH increments were calculated for intervals $\Delta t \approx 15$ s. Zero time ($t=0$) in **b** and **c** corresponds to 530 s from the moment of cell wall incision

of H^+ consumption on the outer side of plasmalemma occurred in parallel with the cyclosis-mediated passage across the AOI of a cytoplasmic portion enriched with reducing equivalents. These data indicate that reducing equivalents carried with the cytoplasmic flow and elevating chloroplast fluorescence F' are implicated in the mechanism of pH increase on the surface of microperforated cells.

Comparison with cyclosis-mediated F' and pH_o changes in the absence of wounding

The above-described experiments were conducted on cell regions producing under light the external acid zones with pH 6.3–6.5. In these cell regions unexposed to microperforation, a slight decrease in pH_o was observed upon application of LL to a distant area located upstream in the cytoplasmic flow (data not shown, but see Fig. 7 in (Bulychev and Komarova 2015)). By contrast, after CW incision, illumination of a remote cell region induced pH changes of the opposite polarity (see Fig. 5).

In *Chara* internodal cells exposed to weak background light, external alkaline zones may arise in preselected cell areas under localized illumination of a distant region (Dodonova and Bulychev 2011). In this case, the narrow beam applied at a distance from the point of measurements induced the increase in pH_o that was preceded by a transient increase in F' fluorescence (Fig. 6a). The position of the fluorescence peak on a time scale coincided with the beginning of alkaline zone formation, the latter process reflects the opening of H^+ (OH^-)-conducting channels (Bisson and Walker 1980; Beilby and Bisson 2012; Beilby and Casanova 2014). When the formation of alkaline zone started from nearly neutral pH_o , as in Fig. 6a, the transition from low to high pH was observed after 200–250 s of LL treatment. When the measurements were performed on cell regions with elevated pH_o , a shorter pulse of LL was sufficient to induce the concurrent increases in F' and pH_o (Fig. 6b). These findings imply that the cyclosis-mediated transport of reducing equivalents might be engaged in some functions apart from the distant regulation of photosynthesis and healing the microwounds.

One matter of concern regarding extracellular pH measurements is that the pH microelectrode might respond to changes in cell membrane potential and extracellular electric fields during dark–light transitions. A question arises as to whether the local illumination of a remote cell region could disturb the readings of pH microelectrodes by affecting the extracellular electric potential. In order to answer this question, we compared the electric potential responses of the pH microsensors and a conventional capillary microelectrode to localized illumination of a remote cell region, when the tips of both electrodes were positioned in close proximity to each other. The results are shown in Fig. 7. It is seen that the potential difference between the pH microelectrode and the reference

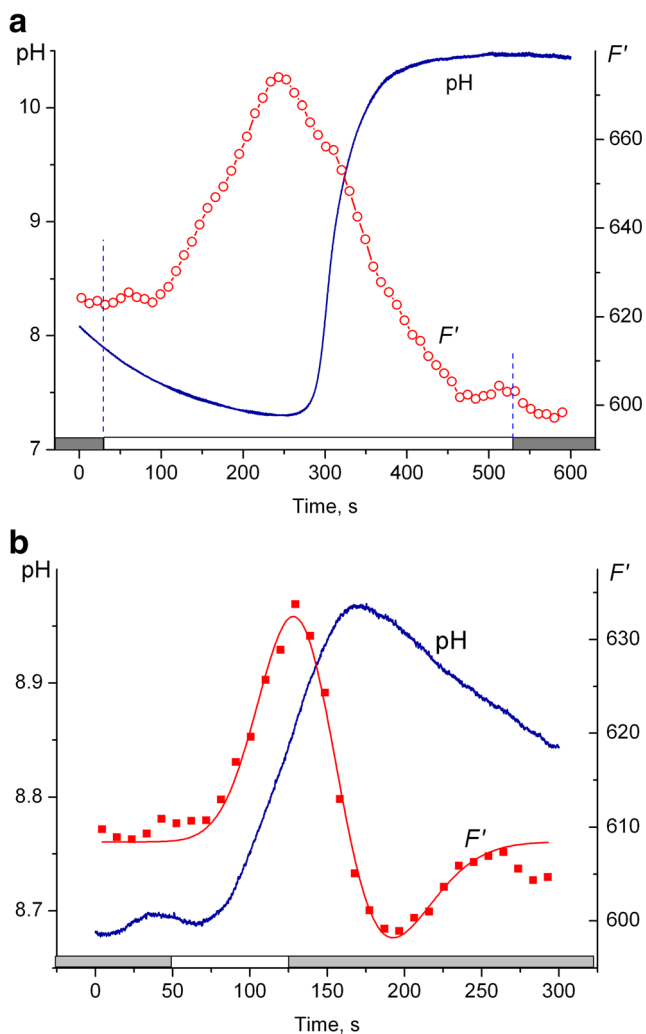


Fig. 6 Changes in chlorophyll fluorescence F' and surface pH (pH_s) in cell regions producing alkaline zones under remote application of LL pulse with a photon flux density $500 \mu\text{mol m}^{-2} \text{s}^{-1}$. **a** Development of alkaline zone under prolonged localized illumination of a remote cell region ($d=1 \text{ mm}$). The timing of LL is depicted by dark/light bars along the time axis. Prior to the onset of recording, the alkaline zone was first pre-formed under intense illumination and then decayed under dim background light toward the neutral or slightly acid pH level. At $t=30 \text{ s}$, the remote LL was switched on, which was followed by restoration of the alkaline zone. Background light intensity was $19.9 \mu\text{mol m}^{-2} \text{s}^{-1}$. Note that a sharp increase in pH was preceded by the transient increase in F' fluorescence. **b** Enhancement of external alkalization under the action of a comparatively short LL pulse (75 s) applied at a 1.5-mm distance on the upstream side of analyzed area; the background irradiance of the whole cell was $17.8 \mu\text{mol m}^{-2} \text{s}^{-1}$. The timing of localized illumination is depicted by dark/light bars along the time axis. Note the transient rise in F' preceding the pH peak

electrode (curve 1) shifted in response to localized illumination of a distant cell region from approximately 45 to -70 mV , which corresponded to the pH increase from 7.0 to 9.2. By contrast, the potential difference between the capillary microelectrode and the reference electrode (curve 2) was largely unaffected by LL and alkaline spot formation. Furthermore,

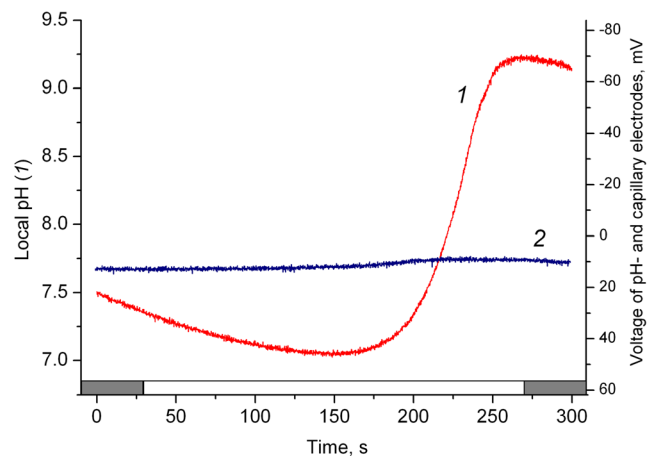


Fig. 7 Potential changes recorded with a pH microelectrode (curve 1) and a capillary microelectrode (curve 2) near the surface of *Chara* internode under localized illumination of a remote cell region. The tips of the two microelectrodes were positioned 1 mm downstream from the center of an optic fiber at a close ($\sim 10 \mu\text{m}$) proximity to each other. The potential differences 1 and 2 were measured with respect to an Ag/AgCl reference electrode contacting the experimental chamber through a flexible agar-filled salt bridge. The background irradiance of the whole cell was $9 \mu\text{mol m}^{-2} \text{s}^{-1}$. The pH values on the left y axis correspond to voltages of the pH microsensors scaled on the right axis. The timing of localized illumination is depicted by dark/light bars along the time axis. A representative experiment for $n=3$ is shown

we performed the electric potential measurements with a capillary microelectrode inserted into the cytoplasm and found out that local illumination of a remote cell region had no appreciable influence on the membrane potential in cells exposed to weak background light (data not shown). Thus, the potential transients recorded with a pH microsensor under the action of LL reflected the dynamics of pH near the cell surface; they were not distorted by extracellular detection of membrane potential changes.

Discussion

Continuous measurements of chlorophyll fluorescence F' at various distances from the locally illuminated region of *Chara* internode revealed the wavelike propagation of F' changes in the direction of cytoplasmic flow at the rates nearly equal to the velocity of cytoplasmic streaming. The increase in F' induced by LL after a distinct lag period indicates the reduction of photosystem II (PSII) quinone acceptor Q_A . The reduction of quinone Q_A presumably results from the entry into the chloroplast stroma of reducing equivalents that are exported in the area of bright illumination from chloroplasts (Foyer and Noctor 2009; Taniguchi and Miyake 2012) and then transferred with the fluid flow (Bulychev and Komarova 2015). The ability of imported stromal NADPH to reduce the plastoquinone pool was deduced from experiments with isolated thylakoids (Endo et al. 1997; Corneille et al. 1998), algae,

and whole leaves (Rumeau et al. 2007). Previous studies revealed the cytoplasmic-mediated transfer of H_2O_2 along the *Chara* internodes from the point of LL application to downstream areas (Eremin et al. 2013). Hydrogen peroxide is known mainly as an oxidizing agent, but it can also exhibit reducing properties. However, the cytoplasmic flow of H_2O_2 cannot account for the increase in chlorophyll fluorescence in downstream cell regions. Neubauer and Schreiber (Neubauer and Schreiber 1989) found that H_2O_2 quenches both actual fluorescence F' (F_t) and the maximal fluorescence F_m in intact spinach chloroplasts by acting as an electron acceptor. Thus, cyclosis-mediated transfer of reducing equivalents in the form of NAD(P)H seems likely.

The height of the transitory peak of F' and the area under the F' curves diminished with the increase in the separation distance d . Assuming that the F' level at each instant during the transient is related to the concentration of active metabolite in the cytoplasm, one may suppose that the metabolite content in the fluid flow declines with the distance from the point of LL application because shaded chloroplasts consume this metabolite during its passage along the shaded cell parts. However, the decrease in metabolite content with the axial distance might be less steep than experimentally observed, if the movement of cytoplasm along a slightly twisted helical path is taken into account. When the light spot is displaced linearly along the internode axis, it illuminates the chloroplasts residing in different streamlines of fluid. Deviation of these streamlines from the center of F' measurements may account for the seeming decrease in F' changes.

Fluorescence induction curves in cell regions directly exposed to LL differed substantially from the F' fluorescence changes recorded at various distances from the intensely lighted area (Fig. 1). These distinctions correspond to different ways of Q_A reduction under the action of straight light and via cyclosis-mediated transport of reducing equivalents. Clearly, the accumulation of NADPH in the stroma of brightly illuminated chloroplasts followed by the export of the reductants into the cytoplasm should differ kinetically from the photochemical reduction of Q_A .

Measurements of continuous F' profiles at various distances from the light spot revealed a previously unnoticed stage of F' changes induced by remote lighting, namely, a fast F' quenching during LL treatment at a space interval of ~ 0.8 mm from the light–shade border. This stage is intriguing as it contributes to the complex influence of remote light on the functional condition of chloroplasts located away from the illuminated area. It cannot be explained by incidence of stray light because even dim irradiance elevates F' by facilitating Q_A reduction. This transient fluorescence quenching was only manifested at a comparatively short distance from the light–shade margin. It is presumably related to circulating electric currents carried by protons and to the formation of acid and

alkaline zones on the border between the illuminated and shaded parts of *Chara* internode, respectively.

The results show that the profiles of F' changes caused by localized illumination of a distant cell region depend on the velocity of cytoplasmic streaming. At low streaming velocities, diffusion of the active intermediate in the axial direction manifested itself in a widened band of F' changes. Using a simplifying assumption that LL elevates the cytoplasmic concentration of the active metabolite in a narrow segment of the internode, we suppose that the shape of F' transients is hardly affected by diffusion at high velocities of cytoplasmic streaming and, conversely, that diffusion is almost unaffected by the fluid flow at low streaming velocities so that Fick's law is applicable. In this case, the longitudinal profile caused by unidirectional diffusion of the active substance during its travel with the retarded flow along the cell toward AOI will conform to the normal distribution with the dispersion $x^2 = 2Dt$, where D is the diffusion coefficient. According to the literature data, the diffusion coefficient of low-molecular substances, such as nucleotides in the cytoplasm is $D_{\text{cyt}} = 3 \cdot 10^{-6} \text{ cm}^2 \text{ s}^{-1}$ (e.g., Kalwarczyk et al. 2012).

Since photosynthetic electron transport of *Chara* chloroplasts is insensitive to cytochalasin D treatment (Sommer et al. 2015), we assume that the times required for the release of active intermediate from chloroplasts into the cytoplasm of illuminated region and for its processing in shaded regions are unaffected by cytochalasin D treatment. Then, the time t during which the diffusion proceeds can be calculated as the difference of F' peak positions at low and fast streaming rates. At the streaming rate of $18 \mu\text{m s}^{-1}$, the F' peak was attained 44 s later than at $75 \mu\text{m s}^{-1}$. The standard deviation caused by diffusion of the intermediate throughout a 44-s period at $D_{\text{cyt}} = 3 \cdot 10^{-6} \text{ cm}^2 \text{ s}^{-1}$ will be $x = (2Dt)^{1/2} = (2 \cdot 3 \cdot 10^{-6} \cdot 44)^{1/2} = 0.0162 \text{ cm} = 162 \mu\text{m}$. The full width of the Gaussian band at a half maximum is related to x by the coefficient $2(2 \cdot \ln 2)^{1/2} = 2.355$. Thus, the calculated widening of the band will be $162 \cdot 2.355 \approx 380 \mu\text{m}$. In the experiment, the difference of F' bandwidths at low and fast streaming velocities was $47 - 26 = 21$ s. By rescaling this widening from units of time to units of length for the streaming velocity of $18 \mu\text{m s}^{-1}$, one can find that the bandwidth of F' transients increased by $378 \mu\text{m}$ in this experiment. Strict coincidence of estimated and experimental values seems accidental, considering the simplifying assumptions adopted. However, the correspondence of estimates and experimental data by the order of magnitude supports the view that a functionally active low-molecular-weight metabolite is transported in an unbound form.

The results of this study provide evidence for the involvement of cyclosis-mediated transport in the pH_o rise around the point of cell wall incision. Simultaneous measurements of chloroplast fluorescence and the cell surface pH at the point of microincision revealed that the arrival of cytoplasm

delivering the photosynthetically active metabolite from the area of intense illumination is accompanied by an additional pH rise in the alkaline area produced after microwounding. The synchronous development of F' and pH_o changes suggests that both processes are mediated by a common intermediate. Simultaneous transfer of two different intermediates featuring equal time of their export into the cytoplasm and identical processing periods in thylakoids and at the plasma membrane is not excluded but seems less likely than the transfer of a shared intermediate.

Reduced nucleotides may act as a substrate for plasma membrane NADPH oxidase that catalyzes the transmembrane electron transport to O_2 with a possible consumption of H^+ on the external cell side. Such coupling of electron transport with the consumption–release of protons was considered in the original chemiosmotic hypothesis with regard to energy-transducing membranes ((Mitchell 2011) republished). It is known that cyanobacteria possess NAD(P)H–oxygen oxidoreductase donating electrons directly to O_2 without production of reactive oxygen species (Helman et al. 2003; Allahverdiyeva et al. 2013). On the other hand, the proton consumption may also result from one-electron reduction of O_2 followed by O_2^- dismutation reaction (Asada 2006). Deeper understanding of the events occurring in the plasma membrane at the site of cell wall wounding can be obtained by analyzing O_2 dynamics in the area of microwounding using oxygen microsensors.

In photosynthetically active cell regions capable of forming external acid zones, the localized illumination of a distant cell part promoted slight lowering of the external pH, whereas the same LL treatment induced the pH_o increase after the cell wall incision. These observations emphasize a specific mechanism of the remote LL action on microperforated cell regions. They present evidence that cytoplasmic streaming carries the intracellular components utilized in the region of CW incision.

Acknowledgments We are grateful to Prof. Ilse Foissner (University of Salzburg) for the gift of cytochalasin D and helpful discussion. This work was supported by the Russian Foundation for Basic Research, project no. 16-04-00318.

Compliance with ethical standards

Conflict of interest The authors declare that they have no conflict of interest.

References

- Allahverdiyeva Y, Mustila H, Ermakova M, Bersanini L, Richaud P, Ajlani G, Battchikova N, Cournac L, Aro E-M (2013) Flavodiiron proteins Flv1 and Flv3 enable cyanobacterial growth and photosynthesis under fluctuating light. *Proc Natl Acad Sci U S A* 110:4111–4116
- Allen NS, Allen RD (1978) Cytoplasmic streaming in green plants. *Annu Rev Biophys Bioeng* 7:497–526
- Asada K (2006) Production and scavenging of reactive oxygen species in chloroplasts and their functions. *Plant Physiol* 141:391–396
- Beilby MJ, Bisson MA (2012) pH banding in charophyte algae. In: Volkov AG (ed) *Plant electrophysiology: methods and cell electrophysiology*. Springer, Berlin, pp 247–271
- Beilby MJ, Casanova MT (2014) *The physiology of characean cells*. Springer, Berlin
- Bisson MA, Walker NA (1980) The *Chara* plasmalemma at high pH. Electrical measurements show rapid specific passive uniprot of H^+ or OH^- . *J Membr Biol* 56:1–7
- Bulychev AA, Dodonova SO (2011) Effects of cyclosis on chloroplast–cytoplasm interactions revealed with localized lighting in Characean cells at rest and after electrical excitation. *Biochim Biophys Acta* 1807:1221–1230
- Bulychev AA, Kamzolkina NA (2006) Differential effects of plasma membrane electric excitation on H^+ fluxes and photosynthesis in characean cells. *Bioelectrochemistry* 69:209–215
- Bulychev AA, Komarova AV (2014) Proton flows across the plasma membrane in microperforated characean internodes: tonoplast injury and involvement of cytoplasmic streaming. *Protoplasma* 251:1481–1490
- Bulychev AA, Komarova AV (2015) Photoinduction of cyclosis-mediated interactions between distant chloroplasts. *Biochim Biophys Acta* 1847:379–389
- Bulychev AA, Komarova AV (2016) Influence of light on the apoplasmic pH in microwounded cells of *Chara corallina*. *Russ J Plant Physiol* 63:46–53
- Bulychev AA, Alova AV, Bibikova TN (2013a) Strong alkalinization of *Chara* cell surface in the area of cell wall incision as an early event in mechanoperception. *Biochim Biophys Acta* 1828:2359–2369
- Bulychev AA, Alova AV, Rubin AB (2013b) Propagation of photoinduced signals with the cytoplasmic flow along characean internodes: evidence from changes in chloroplast fluorescence and surface pH. *Eur Biophys J* 42:441–453
- Corneille S, Cournac L, Guedeney G, Havaux M, Peltier G (1998) Reduction of the plastoquinone pool by exogenous NADH and NADPH in higher plant chloroplasts: characterization of a NAD(P)H–plastoquinone oxidoreductase activity. *Biochim Biophys Acta* 1363:59–69
- Dodonova SO, Bulychev AA (2011) Cyclosis-related asymmetry of chloroplast–plasma membrane interactions at the margins of illuminated area in *Chara corallina* cells. *Protoplasma* 248:737–749
- Endo T, Mi H, Shikanai T, Asada K (1997) Donation of electrons to plastoquinone by NAD(P)H dehydrogenase and by ferredoxin–quinone reductase in spinach chloroplasts. *Plant Cell Physiol* 38:1272–1277
- Eremin A, Bulychev AA, Hauser MJB (2013) Cyclosis-mediated transfer of H_2O_2 elicited by localized illumination of *Chara* cells and its relevance to the formation of pH bands. *Protoplasma* 250:1339–1349
- Foissner I (1988) The relationship of echinate inclusions and coated vesicles on wound healing in *Nitella flexilis* (Characeae). *Protoplasma* 142:164–175
- Foissner I, Wasteneys GO (2007) Wide-ranging effects of eight cytochalasins and latrunculin A and B on intracellular motility and actin filament reorganization in characean internodal cells. *Plant Cell Physiol* 48:585–597
- Foissner I, Wasteneys GO (2012) The characean internodal cell as a model system for studying wound healing. *J Microsc* 247:10–22
- Foyer CH, Noctor G (2009) Redox regulation in photosynthetic organisms: signaling, acclimation, and practical implications. *Antioxid Redox Signal* 11:861–905
- Goldstein RE, van de Meent J-W (2015) A physical perspective on cytoplasmic streaming. *Interface Focus* 5:20150030
- Hardham AR, Jones DA, Takemoto D (2007) Cytoskeleton and cell wall function in penetration resistance. *Curr Opin Plant Biol* 10:342–348
- Heil M (2009) Damaged-self recognition in plant herbivore defence. *Trends Plant Sci* 14:356–363

- Helman Y, Tchernov D, Reinhold L, Shibata M, Ogawa T, Schwarz R, Ohad I, Kaplan A (2003) Genes encoding A-type flavoproteins are essential for photoreduction of O₂ in cyanobacteria. *Curr Biol* 13: 230–235
- Kalwarczyk T, Tabaka M, Holyst R (2012) Biologistics—diffusion coefficients for complete proteome of *Escherichia coli*. *Bioinformatics* 28:2971–2978
- Klima A, Foissner I (2011) Actin-dependent deposition of putative endosomes and of endoplasmic reticulum during early stages of wound healing in characean internodal cells. *Plant Biol* 13:590–601
- Krupenina NA, Bulychev AA (2007) Action potential in a plant cell lowers the light requirement for non-photochemical energy-dependent quenching of chlorophyll fluorescence. *Biochim Biophys Acta* 1767:781–788
- Krupenina NA, Bulychev AA, Roelfsema MBG, Schreiber U (2008) Action potential in *Chara* cells intensifies spatial patterns of photosynthetic electron flow and non-photochemical quenching in parallel with inhibition of pH banding. *Photochem Photobiol Sci* 7:681–688
- Leakey ADB, Scholes JD, Press MC (2005) Physiological and ecological significance of sunflecks for dipterocarp seedlings. *J Exp Bot* 56: 469–482
- Menzel D (1988) How do giant plant cells cope with injury?—the wound response in siphonous green algae. *Protoplasma* 144:73–91
- Mitchell P (2011) Chemiosmotic coupling in oxidative and photosynthetic phosphorylation. *Biochim Biophys Acta* 1807:1507–1538
- Monshausen GB, Bibikova TN, Weisenseel MH, Gilroy S (2009) Ca²⁺ regulates reactive oxygen species production and pH during mechanosensing in arabidopsis roots. *Plant Cell* 21:2341–2356
- Neubauer C, Schreiber U (1989) Photochemical and non-photochemical quenching of chlorophyll fluorescence induced by hydrogen peroxide. *Z Naturforsch* 44c:262–270
- Pearcy RW, Krall JP, Sassenrath-Cole GF (1996) Photosynthesis in fluctuating light environments. In: Baker NR (ed) *Photosynthesis and the environment*. Kluwer, Dordrecht, pp 321–346
- Pickard WF (2003) The role of cytoplasmic streaming in symplastic transport. *Plant Cell Environ* 26:1–15
- Rumeau D, Peltier G, Cournac L (2007) Chlororespiration and cyclic electron flow around PSI during photosynthesis and plant stress response. *Plant Cell Environ* 30:1041–1051
- Shimmen T (2007) The sliding theory of cytoplasmic streaming: fifty years of progress. *J Plant Res* 120:31–43
- Sommer A, Hoeflberger M, Hoepflinger MC, Schmalbrock S, Bulychev A, Foissner I (2015) Convoluted plasma membrane domains in the green alga *Chara* are depleted of microtubules and actin filaments. *Plant Cell Physiol* 56:1981–1996
- Suzuki N, Miller G, Morales J, Shulaev V, Torres MA, Mittler R (2011) Respiratory burst oxidases: the engines of ROS signaling. *Curr Opin Plant Biol* 14:691–699
- Taniguchi M, Miyake H (2012) Redox-shuttling between chloroplast and cytosol: integration of intra-chloroplast and extra-chloroplast metabolism. *Curr Opin Plant Biol* 15:252–260
- Toko K, Chosa H, Yamafuji K (1985) Dissipative structure in the characeae: spatial pattern of proton flux as a dissipative structure in characean cells. *J Theor Biol* 114:125–175
- Verchot-Lubicz J, Goldstein RE (2010) Cytoplasmic streaming enables the distribution of molecules and vesicles in large plant cells. *Protoplasma* 240:99–107